Al-Rafidain J Med Sci. 2025;9(2):256-265.
DOI: https://doi.org/10.54133/ajms.v9i2.2513

Research Article

Formulation and Characterization of Novel Itraconazole-Loaded PLGA Nanoparticles for Potential Topical Delivery

Akar Othman Hamakarim, Twana Mohammed Mohammed Ways*
Department of Pharmaceutics, College of Pharmacy, University of Sulaimani, Sulaymaniyah 46001, Kurdistan Region, Iraq
Received: 15 September 2025; Revised: 14 November 2025; Accepted: 18 November 2025

Abstract

Background: Itraconazole (ITZ) is a potent antifungal drug limited by poor water solubility and systemic side effects when taken orally. Topical administration offers a safer approach; however, efficient penetration through the stratum corneum remains a challenge. ***Objective***: To develop and optimize ITZ-loaded PLGA nanoparticles (NPs) by investigating the effects of polymer type (PLGA 50:50 and 75:25) and stabilizers (Tween-80 and PVA) on the NPs size, PDI, and zeta potential, and to evaluate in vitro drug release of free ITZ and NPs. ***Methods***: NPs were prepared by the nanoprecipitation method and were characterized using DLS for particle size, PDI, and zeta potential; FTIR spectroscopy for confirmation of drug encapsulation; FESEM and TEM for morphological assessment; and in vitro drug release studies. ***Results***: All NP formulations were in the nano-size range. The optimal formulation, containing PLGA 75:25 and 1% Tween-80, had the smallest particle size and lowest PDI, with an encapsulation efficiency of 54.74%, a drug loading capacity of 8.46%, and a yield of 58.77%. FTIR spectroscopy confirmed successful incorporation of ITZ into the PLGA matrix, whereas FESEM and TEM revealed smooth, spherical NPs with uniform distribution and no aggregation. In vitro drug release studies of the NPs demonstrated a biphasic profile: an initial burst followed by a controlled release, as opposed to the rapid release of free ITZ. ***Conclusions***: The NPs were successfully prepared. The optimized ITZ-loaded PLGA nanoparticles showed favorable physicochemical characteristics, efficient encapsulation, and controlled drug release, highlighting potential as a topical delivery system for antifungal therapy.

Keywords: Formulation optimization, Itraconazole, Polymeric nanoparticles, PLGA 75:25.

صياغة وتوصيف جسيمات PLGA النانوية المحملة بالإيتراكونازول لتوصيل موضعي محتمل

الخلاصة

الخلفية: إيتراكونازول (ITZ) هو دواء مضاد للفطريات قوي محدود بضعف ذوبانية الماء وآثار جانبية جهازية عند تناوله عن طريق الفم. يمثل الأستخدام الموضعي نهجا أكثر أمانا؛ ومع ذلك، لا يزال الاختراق الفعال عبر الطبقة القرنية يمثل تحديا. **الهدف**: تطوير وتحسين جسيمات PLGA النانوية المحملة ب ITZ (NPs) من خلال دراسة تأثيرات نوع البوليمر (PLGA 50:50 و75:25) والمثبتات (Tween-80 و PVA) على حجم NPs، وPDI، وإمكانات زيتا، وتقييم إطلاق دواء ITZ وNPs الحرة في المختبر. **الطرائق**: تم إعداد NPs باستخدام طريقة الترسيبات النانوية وتم توصيفها باستخدام DLS لحجم الجسيمات، PDI، وجهد زيتا؛ تحليل طيف FTIR لتأكيد تغليف الدواء؛ FESEM وTEM للتقييم الشكلي؛ ودراسات إطلاق الأدوية في المختبر. **النتائج**: جميع تركيبات NP كانت ضمن نطاق حجم النانو. التركيبة المثلى، التي تحتوي على PLGA 75:25 و1٪ Tween-80، كانت أصغر حجم جسيمات وأقل مؤشر PDI، بكفاءة تغليف تبلغ 54.74٪، وقدرة تحميل دواء 8.46٪، وعائد 58.77٪. أكد مطيافية FTIR نجاح دمج ITZ في مصفوفة PLGA، بينما كشف FESEM وTEM عن NPs كروية ناعمة مع توزيع منتظم وبدون تجميع. أظهرت دراسات إطلاق الأدوية في المختبرات على الممرضين الممرضين مظهرا ثنائي المرحلة: انفجار أولي يتبعه إطلاق محكم، على عكس الإطلاق السريع ل ITZ الحر. **الاستنتاجات**: تم تصنيع الجسيمات النانوية بنجاح. أظهرت الجسيمات النانوية المحسنة ب PLGA المحملة ب ITZ خصائص فيزيائية كيميائية مفضلة، وتغليف فعال، وإطلاق دواء مضبوط، مما أبرز إمكاناته كنظام توصيل موضعي للعلاج المضاد للفطريات.

* ***Corresponding author***: Twana M. Mohammed Ways, Department of Pharmaceutics, College of Pharmacy, University of Sulaimani, Sulaymaniyah 46001, Kurdistan Region, Iraq; Email: twana.mohammed@univsul.edu.iq
Article citation: Hamakarim AO, Mohammed Ways TM. Formulation and Characterization of Novel Itraconazole-Loaded PLGA Nanoparticles for Potential Topical Delivery. *Al-Rafidain J Med Sci*. 2025;9(2):256-265. doi: https://doi.org/10.54133/ajms.v9i2.2513

INTRODUCTION

Itraconazole is a broad-spectrum antifungal agent extensively used for the treatment of superficial and systemic fungal infections, including dermatophytosis and candidiasis [1,2]. Despite its therapeutic efficacy, itraconazole is characterized by poor aqueous solubility and incomplete oral bioavailability, which can limit its clinical performance [3]. Moreover, systemic administration of itraconazole has been associated with adverse effects such as hepatotoxicity and gastrointestinal disturbances [4]. Consequently, alternative strategies, particularly topical skin delivery systems, have gained interest for enhancing localized drug concentrations at the site of infection while minimizing systemic exposure. Topical drug delivery

offers several advantages, including site-specific targeting, improved patient compliance, and reduction of systemic side effects [5]. However, effective topical delivery of itraconazole remains challenging due to the highly effective barrier function of the stratum corneum, the outermost layer of the skin [6,7]. Additionally, itraconazole doesn't dissolve well in either water or fat, which makes it harder for it to get through the skin layers. To make itraconazole work well when applied topically, scientists need to come up with new delivery systems that have features like smaller particles that can get deeper into the skin, keeping the drug from breaking down, and being able to provide sustained drug release. Nanoparticulate drug delivery systems have emerged as promising approaches to overcome the limitations associated with conventional topical formulations. Nanoparticles (NPs) have many benefits, such as making drugs more soluble, protecting them from breaking down, releasing them slowly and steadily, and making it easier for them to pass through the stratum corneum [8–10]. There are many types of nanoparticle systems, but poly(lactic-co-glycolic acid) (PLGA) nanoparticles have gotten a lot of attention because they are biocompatible and biodegradable, and the FDA has approved them for use in pharmaceutical products. When PLGA nanoparticles are used to hold hydrophobic drugs like itraconazole, they can provide a controlled release profile that could improve the effectiveness of topical antifungal therapy [11–14]. In the development of nanoparticulate systems for topical delivery, it is critical to optimize key formulation parameters that govern stability, skin interaction, and drug release behavior. Particle size and polydispersity index (PDI) influence the uniformity and penetration ability of nanoparticles, while zeta potential affects colloidal stability [15]. Moreover, understanding the drug release profile and releasing kinetics from nanoparticles is fundamental to predicting *in vivo* performance. So, systematic optimization and physicochemical characterization of itraconazole-loaded PLGA nanoparticles are important first steps toward making a system that can effectively deliver itraconazole to the skin. Although nanoparticle-based strategies have been explored for itraconazole delivery, previous studies have been limited to the use of PLGA 50:50 as the polymeric carrier, with minimal investigation into the effects of varying polymer and stabilizer types [16,17]. In contrast, the present study systematically evaluates itraconazole-loaded PLGA nanoparticles prepared with both PLGA 50:50 and PLGA 75:25, providing a comparative assessment of their physicochemical properties. Furthermore, while polyvinyl alcohol (PVA) has been commonly used as a stabilizer in earlier formulations, the incorporation of Tween 80 at varying concentrations (1% and 2%) represents a novel approach to modulating nanoparticle characteristics. Not only does this study find the best mixture of PLGA 75:25 and Tween 80, but it also gives a full description of the particle size, surface shape, ability to encapsulate, and drug release behavior in vitro. To the best of our knowledge, this is the first systematic investigation to explore the combined effects of polymer and stabilizer types on the properties of itraconazole-loaded PLGA nanoparticles, offering new insights for the design of topical antifungal delivery systems. The present study aims to formulate and optimize itraconazole-loaded PLGA nanoparticles and to characterize their physicochemical properties, including particle size, PDI, and zeta potential. The optimized nanoparticles' ability to encapsulate drugs, *in vitro* drug release behavior, and their release kinetics were also studied. The effects of polymer type (PLGA 50:50 versus PLGA 75:25) and stabilizer type and concentration (PVA and Tween 80) on the formulation characteristics are systematically investigated to identify an optimized nanoparticle system for potential topical skin delivery. The findings of this study will pave the way for future research on the use of these nanoparticles in topical antifungal therapy.

METHODS

Materials

PLGA 50:50, PLGA 75:25, and itraconazole were purchased from Kemprotec Limited (UK). Tween 80 (Sigma-Aldrich, UK); PVA (BIOCHEM Chemopharma, France); acetone (Carlo Erba Reagents, Italy); ethanol (Merck, Germany); cellulose dialysis membrane (MWCO 14 kDa, Membra-Cell, USA); acetonitrile (Merck, Germany); and dimethyl sulfoxide (DMSO, BIOCHEM Chemopharma, France) were also used.

Preparation of ITZ-loaded nanoparticles

PLGA nanoparticles, both ITZ-loaded and blank (without ITZ), were prepared using the nanoprecipitation method. This technique consists of two basic steps: the first step is the preparation of the organic and aqueous phases, and the second step is the controlled addition of the organic phase into the aqueous phase that allows nanoparticle production. The identical process was performed for blank nanoparticles, except that ITZ was eliminated from the formulation. To appropriately wet and swell the polymer, 100 mg of PLGA was precisely measured and dissolved in 10 mL of acetone while being stirred at 600 rpm for 15 minutes. After that, the solution was stirred for a further 15 minutes while 10 mg of ITZ was added. The identical process was used for the blank nanoparticles, with the exception that the formulations did not contain ITZ. A stabilizer (Tween 80 or PVA) was added to 20 mL of 10 mM citrate buffer (pH 5) and stirred for 15 minutes prior to the addition of the organic phase. Two different stabilizer concentrations were employed, including Tween 80 at 1% and 2% and PVA at 0.3% and 1%, depending on the formulation's requirements. Following the preparation of both phases, an infusion pump was used to add the organic phase dropwise into

the aqueous phase at a predetermined rate of 0.5 mL/min. To aid in the fabrication of nanoparticles, the mixture was stirred for 4 hours at 300 rpm. Then the resultant nanoparticles were kept at 2 to 8 °C until further analysis.

Formulation development and optimization

Several preliminary formulations were prepared by varying the drug-to-polymer ratio, different stabilizer concentrations (Tween 80 and PVA), and the organic-to-aqueous phase ratio. These formulations were evaluated visually to assess general appearance and physical stability, including clarity, homogeneity, and phase separation. The results were then used to determine optimal formulation parameters for the preparation of samples intended for further studies. Following the determination of the optimal formulation parameters, several main formulations were prepared, and among them the optimal formulation was selected based on the smallest particle size and PDI. The optimal formulation was then used for further characterization studies, including encapsulation efficiency, drug loading, yield, Fourier transform infrared spectroscopy (FTIR), field emission scanning electron microscopy (FESEM), transmission electron microscopy (TEM), and in vitro drug release behavior.

Characterization of PLGA-NPs

To find out the nanoparticles' diameter and zeta potential, a Zetasizer Nano ZS (Malvern Instruments Ltd., UK) was used in a dynamic light scattering (DLS) study. The nanoparticles were diluted in distilled water at a 1:100 ratio, which was used as the dispersion medium. Particle size measurements were performed at a constant scattering angle of 90° and a controlled temperature of 25 °C. Each sample was analyzed in triplicate. Zeta potential measurements were conducted utilizing a disposable cell packed with carbon-coated electrodes. The electrophoretic mobility data were transformed into zeta potential using the Smoluchowski model (Fκa= 1.5). The shape and surface texture of the nanoparticles were studied using a TESCAN MIRA3 FESEM (Brno, Czech Republic). One drop of the nanoparticle suspension was placed on an aluminum stub (TAAB Laboratories Equipment, Aldermaston, UK) utilizing a double-sided sticky tab (TAAB Laboratories Equipment) and, following drying, was vacuum-coated with gold–palladium in an argon atmosphere for 60 seconds. Imaging was conducted at an accelerating voltage of 15 kV. Particle size was measured from FESEM images using ImageJ 1.54g software, and the particle size distribution graphs were generated using OriginPro software (version 2018 SR1, b9.51.195, OriginLab Corporation, Northampton, MA, USA). TEM (Carl Zess_EM1OC, Germany) was used to examine the morphology of the ITZ-loaded PLGA NPs at a 100 kV accelerating voltage. One drop of NP suspensions was applied on a copper grid coated with carbon and allowed to dry at room temperature for one minute. The sample was then stained with uranyl acetate solution and left to air dry. Then, TEM imaging was conducted. Particle size was measured from the TEM images using ImageJ software (version 1.54g). For yield, encapsulation efficiency, and drug loading, first, the nanoparticles were precipitated and separated from free ITZ, and samples of the optimized formulation were centrifuged. A Maanlab HC 02R centrifuge (Sweden) was used to conduct centrifugation for 40 minutes at 2 °C and 15,000 rpm. The resultant precipitates were freeze-dried using a Biobase BK-FD10P lyophilizer (China) for 48 hours at -20 °C.

The yield of the NPs was calculated using equation 1 [18].

$$\textbf{Yield \%} = \frac{\textit{Mass of the nanoparticles recovered} \times 100}{\textit{Mass of polymeric material and drug in the formulation}} \quad (1)$$

A weighed quantity of lyophilized NPs was dissolved in ACN, vortexed for 5 min, and then stirred for 1 hr to ensure a full and complete dissolution. Then a UV/visible spectrophotometer (PharmaSpec, UV-1700, Japan) was used to detect the ITZ absorbance at a wavelength (λ_{max}) of 265 nm. An ITZ calibration curve in ACN solution was used to calculate the concentration of ITZ over the concentration range of 100 to 0.78 µg/mL. The EE% and DL% were calculated using equations 2 and 3 [16].

$$\text{EE\%} = \frac{\textit{Amount of ITZ loaded in NPs(mg)}}{\textit{Total amount of ITZ used (mg)}} \times 100 \quad (2)$$

$$\text{DL\%} = \frac{\textit{Amount of ITZ loaded in NPs(mg)}}{\textit{Total amount of formulation (mg)}} \times 100 \quad (3)$$

FTIR spectroscopy was conducted using a Shimadzu FTIR-8400S spectrometer (Shimadzu Corporation, Japan). The analysis was performed on the pure ITZ, polymers, and the lyophilized nanoparticles. The materials were mixed with potassium bromide (KBr) pellets using a mortar and pestle. The FTIR spectra were collected over the wavenumber range of 4000-400 cm^{-1}, 3 scans with a resolution of 2 cm^{-1}.

In vitro drug release

The dialysis membrane method was used to study the drug release of ITZ and ITZ-loaded PLGA nanoparticles in a lab setting. Thirty grams of freeze-dried nanoparticles were mixed with two milliliters of a 1:1 mixture of DMSO and 0.005 M phosphate-buffered saline (PBS, pH 5) with 1% v/v Tween 80. This was the same as adding 1.25 mg/mL of ITZ. It was put into a cellulose dialysis membrane (MWCO 14 kDa, Membra-Cell, USA) that had been soaked in water overnight and washed several times with the release medium before it was used. The dialysis membrane was firmly tied at both ends using a clamp, and its center part was immersed in

40 mL of the release medium (1:1 DMSO and 0.05 M PBS, pH 5, with 1% Tween 80) kept at 32 ± 1°C under constant stirring at 100 rpm. At predetermined time intervals, 5 mL of the external dialysis medium was removed and quickly replaced with an equal amount of fresh release medium to keep sink conditions. An ITZ solution at 1.25 mg/mL in a liquid mixture of water and DMSO (1:3 v/v) was used as a reference [19]. The concentration of ITZ in the collected samples was measured using UV-visible spectrophotometry at a maximum wavelength (λ_{max}) of 262 nm, based on a calibration curve constructed using a 3:1 ethanol:water mixture over the concentration range of 100 µg/mL to 0.78 µg/mL. The experiment was performed in triplicate.

Drug release kinetics

The *in vitro* release kinetics of PLGA NPs were analyzed using the DDSolver software program [20, 21]. The DDSolver program uses a built-in library of 40 dissolution models to examine release data through nonlinear optimization methods. Model performance and goodness of fit were measured based on the coefficient of determination (R^2), Akaike Information Criterion (AIC), and Model Selection Criterion (MSC). Due to its high R^2 value, low AIC, and high MSC score, the model that best describes how ITZ-loaded PLGA nanoparticles are released was chosen. In addition, the DDSolver software was used to determine the similarity factor (f_2), which was used to analyze the difference between ITZ released from PLGA NPs and free ITZ. An f_2 value greater than 50 usually shows no significant difference between the two release profiles ($p > 0.05$), whereas an f_2 value less than 50 indicates a statistically significant difference ($p < 0.05$) [20, 22].

Stability study

Physical stability of the optimized ITZ-loaded PLGA nanoparticles was evaluated by assessing both the visual appearance of the nanoparticle formulation for the freshly prepared nanoparticles and those stored in the fridge at 4°C for a month to detect any changes in physical appearance, such as color change or precipitation. In addition, the size and PDI of the optimized formulation were measured using DLS (Malvern Instruments, UK) for both the fresh and stored formulations to assess any potential changes in size distribution over time.

Ethics considerations

This study was performed according to the standard procedures and institutional guidelines, and the study protocol was reviewed and approved by the Ethics and Research Registration Committee at the College of Pharmacy, University of Sulaimani (approval number PH144-24).

Statistical analysis

All tests were done in triplicate, and the results are reported as mean ± standard deviation, which were calculated using Microsoft Excel software 2021 (version 2503). Statistical analysis was carried out with the independent t-test by utilizing IBM SPSS Statistics (version 25) software together with the DDSolver program. A *p*-value of < 0.05 was considered statistically significant.

RESULTS

Drug-free nanoparticles and non-optimized and optimized nanoparticles were prepared, and their physical appearance as well as their size was evaluated. Figure 1 shows the general appearance and comparative size and PDI of the blank, non-optimized, and optimized formulations. Based on physical appearance, drug-free nanoparticles showed no precipitation. The non-optimized NPs showed a relatively large volume of precipitation, while the optimized NPs showed almost no or minimum precipitation. The particle size of the blank NPs was 132 nm, non-optimized ITZ-loaded PLGA NPs was 104 nm, and optimized ITZ-loaded PLGA NPs was 135 nm. The optimal parameters for the main formulations consisted of a drug-to-polymer ratio of 1:10, Tween 80 concentrations of 1% and 2%, PVA concentrations of 0.3% and 1%, and an organic solvent-to-aqueous phase ratio of 1:2.

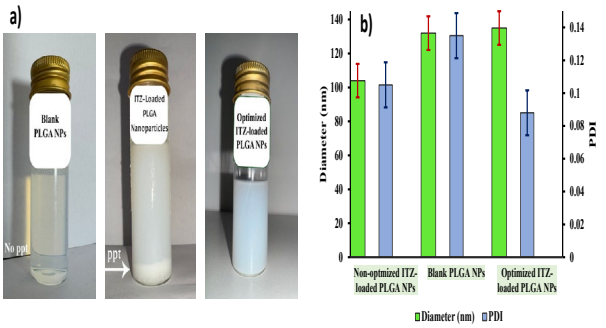

Figure 1: **a)** General appearance, and **b)** particle size and PDI of the blank PLGA NPs, non-optimized ITZ-loaded PLGA NPs and optimized ITZ-loaded PLGA NPs formulation.

To assess the influence of polymer type on nanoparticle formulations, one set of formulations was created with PLGA 50:50, while the other set employed PLGA 75:25. The components of the main formulations are shown in Table 1.

Table 1: Composition of the Main ITZ-Loaded PLGA Nanoparticle Formulations

Formula	ITZ (mg)	PLGA 50:50 (mg)	PLGA 75:25 (mg)	Tween-80 (%)	PVA (%)	Organic phase (mL)	Aqueous phase (mL)
F0	0.0		100	1		10	20
F1	10	100		1		10	20
F2	10	100		2		10	20
F3	10	100			0.3	10	20
F4	10	100			1	10	20
F5	10		100	1		10	20
F6	10		100	2		10	20
F7	10		100		0.3	10	20
F8	10		100		1	10	20

The DLS results (size, PDI, and zeta potential) for all main formulations are presented in Table 2. All the nanoparticle formulations were in the nano size range, ranging from 135 ± 1.6 to 252 ± 2.2 nm. The PDI value of formulations was between 0.088 ± 0.013 and 0.306 ± 0.03, which indicates a good uniformity of the formulations and was considered acceptable. Considering zeta potential, most formulations revealed a value around -10 mV.

Table 2: Physicochemical properties of the main ITZ-loaded PLGA nanoparticles (n=3)

Formula	Z-average (d.nm)	PDI	Zeta potential (mV)
F1	156±2.9	0.108±0.016	-10±1.07
F2	163±4.6	0.163±0.02	-7±0.2
F3	170±1.9	0.128±0.01	-8.9±0.3
F4	252±2.2	0.178±0.02	-18.8±0.7
F5	135±1.6	0.088±0.013	-11±1.1
F6	138±6.7	0.137±0.008	-7±0.6
F7	201±9.9	0.306±0.03	-17±4.3
F8	141±5.9	0.103±0.006	-16±2.0

Values are expressed as mean±SD.

The type of PLGA used in the formulation of the nanoparticles had a statistically significant effect (p< 0.041) on the size of the NPs. Similarly, the type of stabilizer (Tween 80 *vs*. PVA) significantly (p< 0.003) influenced the size of the NPs. However, the difference in NP size between the two concentrations of Tween 80 (1% vs. 2%) was not statistically significant (p> 0.544), nor was the difference between the two concentrations of PVA 0.3% vs. 1% (p> 0.678). No significant difference in zeta potential value between different PLGA types (p> 0.415) and also two different PVA concentrations (0.3% and 1%) (p> 0.057) was observed. However, different stabilizer types (Tween 80 and PVA) and also different Tween 80 concentrations (1% and 2%) had significantly affected zeta potential (p< 0.0001 and p< 0.0002, respectively). Particle size distributions for formulations F1 to F8 showed a uniform distribution of the particles, as shown in Figure 2. The optimal formulation was determined based on the parameters of the smallest nanoparticle size and the lowest PDI, both indicating greater uniformity and stability. Among the evaluated formulations, F5 displayed the most desirable features, having a size of 135 ± 1.6 nm and the lowest PDI of 0.088. Therefore, further investigations were performed on the optimal formulation to evaluate its performance and stability. Figure 3 shows the FTIR spectrum of pure ITZ. It had distinctive peaks at about 3000 cm^{-3}, which means the –NH_2 stretching, and at 2974 cm^{-3}, which means the =C–H stretching of the aromatic ring. Additionally, a peak at 1700 cm^{-1} was identified for C=O stretching, while two peaks at 1614 cm^{-1} and 1500 cm^{-1} related to C=C stretching of the aromatic ring.

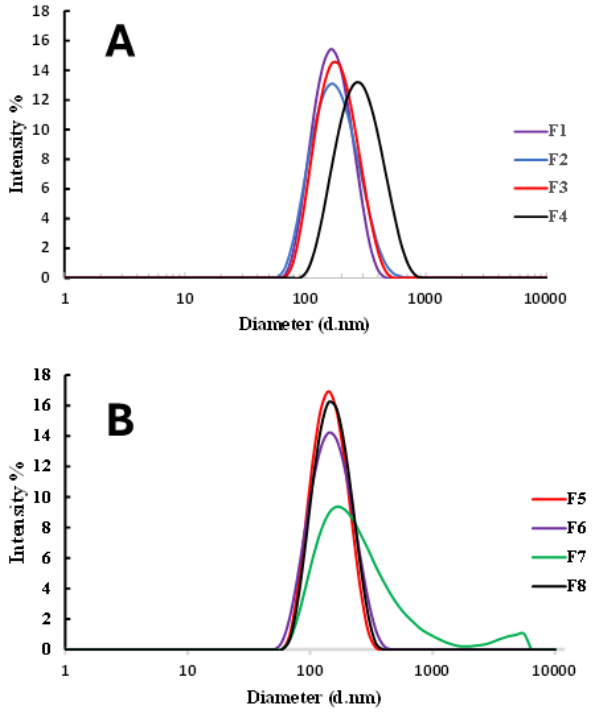

Figure 2: DLS size distribution of the main ITZ-loaded PLGA nanoparticle formulations, **A)**: F1 to F4 prepared using PLGA 50:50, and **B)**: F5 to F8 prepared using PLGA 75:25.

A peak at 1045 cm^{-1} was also found, corresponding to the C–O functional group in ITZ. The FTIR spectrum of PLGA polymer showed a signal at around 3500 cm^{-3}, which was caused by –OH stretching, and a peak at 1750 cm^{-3}, which showed the presence of a carbonyl (C=O) group. The FTIR spectrum of PLGA nanoparticles loaded with ITZ showed clear peaks from both ITZ and PLGA. This spectrum exhibited a peak at 3500 cm^{-1} for the –OH stretching of PLGA, alongside a doublet peak around 3100 cm^{-1}, corresponding to the –NH_2 stretching of ITZ. In addition, a peak at 1750 cm^{-1} was detected,

showing the C=O stretching of both ITZ and PLGA. A signal at 1080 cm^{-1} was also observed, corresponding to C–O stretching of ITZ.

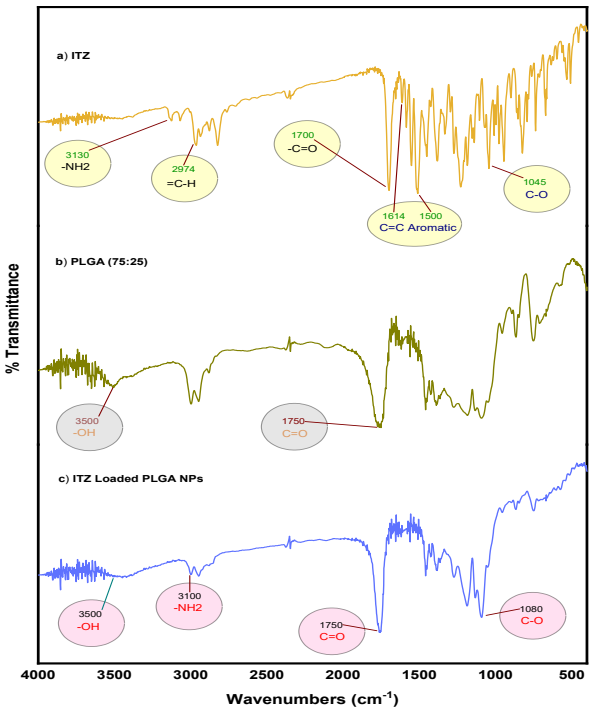

Figure 3: FTIR spectrum. **a)** ITZ, **b)** PLGA 75:25, and **c)** ITZ-loaded PLGA nanoparticles.

The yield of the nanoparticles was 58.77% ± 0.75%. The encapsulation efficiency (EE %) and drug loading (DL %) were found to be 54.74% ± 0.52% and 8.46% ± 0.05%, respectively. The FESEM images (Figure 4a) illustrate the morphological characteristics and surface properties of nanoparticles. The results demonstrate a homogeneous distribution of particles over the area with a relatively narrow distribution. Most of the nanoparticles appeared distinct, approximately spherical in shape, and displayed a smooth surface appearance. No apparent aggregation was detected, which indicates a stable dispersion.

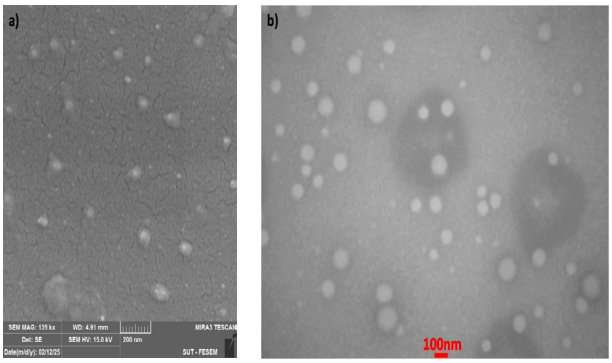

Figure 4: **a)** Field Emission Scanning Electron Microscopy (FESEM) images of the optimal ITZ-loaded PLGA nanoparticles; **b)** Transmission Electron Microscopy (TEM) images of the optimized ITZ-loaded PLGA formulation.

Figure 5a shows that the best-sized ITZ-loaded PLGA NPs were 73.24 ± 32.4 nm, which was found in the FESEM study. The TEM images (Figure 4b) show the morphological and surface characteristics of the nanoparticles. Similar to the FESEM data, the results showed that most of the particles were nearly spherical and looked separate. The particles were spread out evenly across the area with a fairly narrow distribution, and they didn't seem to be sticking together, which suggests that the particles were spread out steadily. We did TEM analysis (Figure 5b) along with FESEM and got similar results. The particle size from TEM was 76.27 ± 26.4 nm, while the particle size from FESEM was 73.24 ± 32.4 nm.

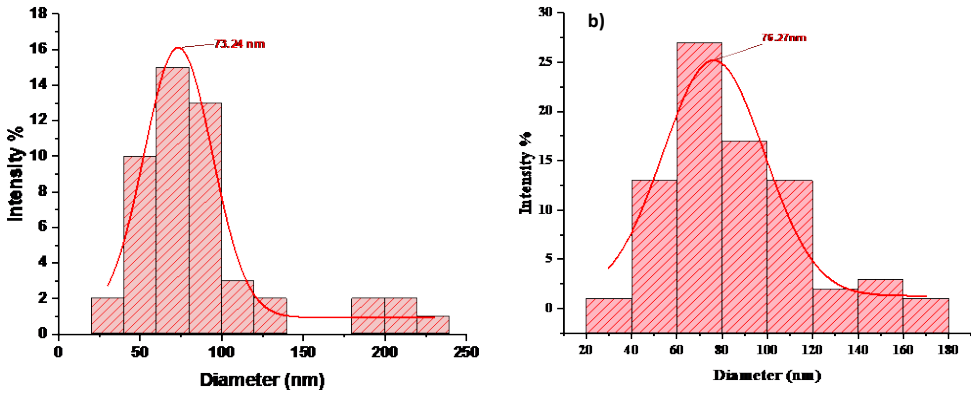

Figure 5: **a)** FESEM-derived particle size distribution curve and histogram of the of the optimized ITZ-loaded PLGA nanoparticles based on FESEM analysis; **b)** TEM-derived size distribution curve and histogram of the optimized ITZ-loaded PLGA nanoparticles based on TEM analysis.

The drug release profile of free drug and ITZ-loaded PLGA NPs was determined**.** The percentage of cumulative drug release from free ITZ solution and ITZ-loaded PLGA NPs is displayed in Figure 6a. Since ITZ is poorly soluble in PBS, Tween 80 was added to the release medium to assure sink conditions. The absorbance of the samples that were collected was used to measure the drug concentrations at different time intervals. A calibration curve established with a 3:1 ethanol-to-water mixture was used for quantification. The DDSolver tool was

employed to model in vitro drug release data and to assist the evaluation of similarities between the release profiles. Table 3 shows the results of parameters of goodness of fit (coefficient of determination, Akaike information criterion, and model selection criterion), which are the important criteria to determine the model of drug release kinetics of the NPs. Also, the values k_1 and k_2 from the equation of the Peppas-Sahlin model were determined to be 0.550 and 0.026, respectively. While the m value is 0.486. As shown in Figure 6b, the predicted drug release profile from the Peppas-Sahlin model is shown along with the observed NPs release profile. The DDSolver tool was used to find the similarity factor (f_2) by comparing how ITZ released from PLGA nanoparticles to how ITZ released on its own. An f_2 value of 31.32 was found, showing a significant difference in the dissolution profiles ($p< 0.05$).

Table 3: DDSolver release data kinetic models to assess the release behavior of ITZ from PLGA NPs

Release Data Models	Parameters of Goodness of Fit		
	R^2 (Highest)	MSC (Highest)	AIC (Lowest)
Zero-order	0.9836	3.9006	75.0974
First-order	0.9792	3.6630	78.1866
Higuchi	0.9519	2.8230	89.1067
Korsmeyer-Peppas	0.9967	5.3407	56.3771
Hixson-Crowell	0.9902	4.4094	68.4841
Peppas-Sahlin	0.9974	5.4232	55.3041

R^2: Coefficient of determination; AIC: Akaike Information Criterion; MSC: Model Selection Criterion.

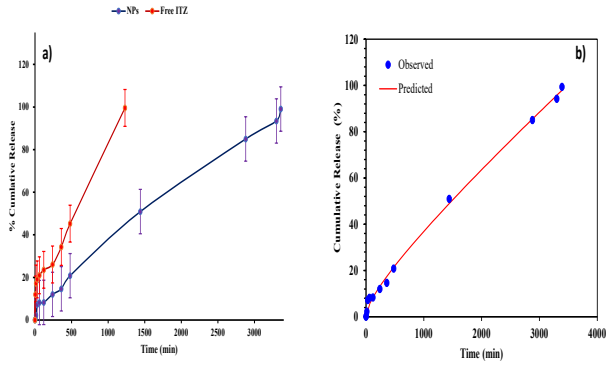

Figure 6: **a)** In vitro drug release profiles of free ITZ solution and ITZ-loaded PLGA NPs; **b)** Predicted and observed in vitro drug release profile of ITZ-loaded PLGA NPs.

To evaluate the physical stability of the optimized ITZ-loaded PLGA nanoparticle formulation, visual inspection was conducted on both the freshly prepared sample and the same formulation after storage at 4 °C for one month. The visual appearance showed no significant change in color; both samples exhibited a similar light blue color. Regarding the precipitation, the freshly prepared optimized formula had no or minimal precipitation, whereas slight precipitation was observed after one month of storage. The same optimized formula was also studied by comparing the size and PDI of the freshly prepared NPs and after one month. The size of freshly prepared NPs was about 135.4 nm, and it changed to 224.5 after one-month storage. Additionally, the PDI of freshly prepared NPs was 0.088, and it has changed to 0.315.

DISCUSSION

In the present study all the main nanoparticle formulations were successfully prepared, where all the nanoparticles were in the nano-sized range. In addition, a new ITZ-loaded PLGA nanoparticle formulation was created. The nanoparticles were then thoroughly characterized in terms of their appearance, particle size, shape, drug release, and stability. The size as well as zeta potential of nanoparticles are critical physicochemical characteristics that substantially affect formulation stability, drug release kinetics, and cellular uptake efficiency [15]. The blank PLGA nanoparticles, which were prepared in the same preparation condition without using ITZ, unsurprisingly had the smallest size (131.8 nm) compared to all main formulations. Findings from the current study reveal that drug-loaded nanoparticle formulations generally display greater particle sizes in comparison to their blank counterparts. This increase in size is mostly linked to the encapsulation of the active pharmaceutical ingredient by high-molecular-weight compounds, such as polymers, which leads to the overall enlargement of the nanoparticle structure during formulation [23]. The blank PLGA nanoparticles exhibited a PDI of 0.135, which is close to that of most formulations and indicates a uniform particle dispersion. When comparing the effect of surfactants on the size of the nanoparticles, in both PLGA 50:50 and PLGA 75:25, the use of Tween 80 consistently resulted in the formation of smaller particles compared to the same formulations using PVA stabilizer. Notably, the F8 had a smaller particle size compared to F1 and F2 but still larger than its Tween counterpart (F5 and F6), indicating the effect of PLGA types on the particle size alongside surfactant types. The results revealed that the use of Tween 80 at both concentrations and in both PLGA types outperformed PVA in reducing the particle size. The particle size distribution curves for all formulations (except F7) showed a unimodal pattern, indicating a relatively narrow and uniform size distribution centered around a predominant peak. Regarding the PDI, the results showed that the use of PLGA 75:25 and a lower concentration of Tween 80 will result in a smaller PDI value and better particle uniformity. F5 had the lowest PDI, which suggests that Tween 80, even at a lower concentration, was more successful in producing a more uniform particle dispersion compared to PVA at a higher concentration, specifically when they were used with PLGA 75:25. Zeta potential is an important parameter for examining the stability of the particles. A high zeta potential enhances electrostatic repulsion and promotes more particle stability, reducing aggregation over a longer duration [24, 25]. F4, F7, and F8 produced the highest zeta values among all other formulations,

indicating better stability of particles. The zeta potential of other formulations was around -10 mV. In the case of F5, where the zeta potential is -11 mV and the dispersion is stable and uniformly dispersed, this can be because of Tween 80, which produced a protective layer around the particles and prevented particle aggregation. The lowest PDI and the smallest particle size of F5 among all other formulations would further confirm that steric stabilization had successfully stabilized the particles and prevented their aggregation. It should be considered that the adsorbed layer of polymers and Tween 80 would shift the plane of shear away from the surface of the particle, which results in a reduction of measured zeta potential. This concludes that even in the case of highly charged particle surfaces, a relatively low zeta potential would be measured, beside this low zeta potential, the systems could be physically stable [26]. Patel *et al*. [17] prepared ITZ-loaded PLGA nanoparticles (size 232 nm, PDI of 0.213, and zeta value of -31.5 mV) using PLGA 50:50 and PVA 0.3% as polymer and stabilizer, respectively. In comparison to their study, the nanoparticles prepared in our study using slightly similar conditions (F3) were smaller and had a lower PDI but had a lower zeta potential. This may be due to the higher molecular weight of PVA (used in our study compared to the PVA used in Patel *et al*.'s study), which would result in a thicker steric layer and may hinder the effective measurement of zeta potential. Although 1% PVA with PLGA was used in literature to form nanoparticles, there were no studies reporting size analysis data with DLS (only with TEM size analysis) to compare with our findings with DLS size analysis data. To the best of our knowledge, this is the first study that reports the use of PLGA 75:25 in combination with Tween 80 as a stabilizer in the formulation of the ITZ-loaded PLGA nanoparticles. While a few studies have explored the use of different PLGA ratios and alternative stabilizers, none have investigated this specific combination. In our study, F5 exhibited a particle size of 135 nm and a PDI of 0.088, which were smaller than those reported by Alhowyanah *et al*. [16], who prepared PLGA nanoparticles with a particle size of 176 nm and a PDI of 0.212 using PLGA 50:50 and D-α-Tocopherol polyethylene-glycol succinate-1000 as a stabilizer. The smaller size and lower PDI observed in our formulation may be attributed to both the polymer composition and the choice of surfactants. Specifically, the use of PLGA 75:25, which is more hydrophobic than PLGA 50:50, in combination with Tween 80, likely contributed to the reduced particle size and improved particle dispersion uniformity compared to previous studies. The FTIR spectrum of ITZ-loaded PLGA nanoparticles exhibited distinctive peaks from both ITZ and PLGA. These findings reveal that the distinctive peaks of both ITZ and PLGA exist in the FTIR spectrum of the nanoparticles, demonstrating a successful formation of the nanoparticles and effective encapsulation of ITZ into PLGA nanoparticles. The yield of the nanoparticles indicates a relatively efficient and reproducible production process. This yield suggests that the formulation and processing parameters were appropriately optimized. And the encapsulation efficiency of the optimal formula indicates a good incorporation of the ITZ into the NPs. The FESEM results prove that the negative zeta potential of the optimal formulation probably provided adequate repulsive forces among the particles, leading to the stability of the system. Furthermore, the majority of nanoparticles falling within a similar size range confirm the low PDI value of 0.088, demonstrating the excellent uniformity and homogeneity of the formulation. The TEM images further confirmed both the relatively small PDI and also the negative zeta potential of the optimal formula, which was able to keep the particles stable and prevented particle aggregation. However, the particle sizes obtained from both FESEM and TEM differed from those measured by DLS (135 ± 1.6 nm), which could be attributed to the differing measurement principles of these techniques. The difference in nanoparticle size measurements is expected, since the DLS analysis was performed on NP suspensions in a completely hydrated and swollen condition, which normally results in greater size values due to the inclusion of solvation layers and possible interparticle interactions. In contrast, FESEM and TEM analyses were performed on air-dried and dehydrated samples, therefore representing the real solid-state dimensions of the nanoparticles. The variation in sample preparation and measurement procedures accounts for the observed variability in particle size. Similar findings have been observed in the literature, further confirming the FESEM and TEM results found in the present study [27]. Regarding the drug release profile of the free ITZ and ITZ-loaded PLGA NPs. ITZ-loaded nanoparticle formulation revealed a biphasic drug release profile. An initial fast release phase was observed within the first 8 hours, during which about 20% of the encapsulated ITZ was released. This burst release is likely attributable to the desorption of drug molecules that were weakly attached to or near the surface of the nanoparticles [28]. It is widely reported that the release rate of drugs from PLGA-based systems is controlled by the lactide-to-glycolide ratio inside the copolymer. A larger lactic acid content enhances the hydrophobicity of the polymer, hence limiting water penetration and slowing down both diffusion and hydrolytic breakdown of the matrix [29]. In the present study, PLGA with a 75:25 lactide-to-glycolide ratio was utilized, which has a higher lipophilic nature than the typically used PLGA 50:50. As a result, a slower and more sustained release pattern was observed, matching with the polymer's higher lactic acid content. After the initial burst phase, a sustained and controlled release of ITZ was observed during the 56 hours, with almost complete release occurring at the 56-hour period. On the other hand, the free ITZ solution revealed total drug release after 20 hours, possibly due to the fast diffusion of the free ITZ molecules across the dialysis membrane. This significant

distinction illustrates the prolonged release characteristic of the ITZ-loaded PLGA nanoparticles compared to the free drug. Drug release kinetics was analyzed by using the DDSolver tool [20, 21], which identified the Peppas–Sahlin model as the most suitable model for explaining the release of ITZ from the PLGA nanoparticle formulation, as it resulted in the highest $R^2 = 0.9974$ and MSC = 5.4232, alongside the lowest AIC = 55.3041. The notably high value of k_1 (0.550) (k_1 and k_2 from the equation of the Peppas-Sahlin model) in comparison with k_2 (0.026) shows that Fickian diffusion is the primary mechanism driving the drug release. The small contribution of k_2 shows little participation of polymer relaxation or degradation [30]. This matches the slow-degrading and hydrophobic properties of PLGA (75:25). Also, m=0.486, which is extremely near to 0.5, indicating that the release mechanism is predominantly diffusion-dominated but with a little contribution from polymer matrix erosion [31]. The similarity factor (f_2) was found to be 31.32. This data demonstrates that the PLGA 75:25 polymer matrix considerably slows down the release of ITZ from the PLGA nanoparticles. Finally, the visual examination of the physical stability of the optimal formula showed no significant change in color between the two samples, while a slight precipitation was observed in the sample after one month of storage, which may be attributed to particle aggregation over time, leading to eventual sedimentation. Also, the results of the size and PDI of the freshly prepared NPs and after one month showed a change in the size from 135.4 nm to 224.5, which was still in the nano-size range, which could indicate the stability of the particles. Additionally, the PDI of freshly prepared NPs was 0.088, and it has changed to 0.315. The increase in PDI is related to the aggregation of the particles and the formation of larger particles (as the size increased) and eventually led to some precipitation. A PDI value of 0.315 is generally considered acceptable, indicating that the nanoparticles have relatively uniform size distribution and potentially good colloidal stability.

Study limitations

Although this study provides significant insights into the formulation and optimization of novel itraconazole-loaded PLGA nanoparticles, several features require further study. The study focused primarily on physicochemical characterization and in vitro release behavior, establishing a strong base for further biological study of itraconazole. However, further studies on long-term stability, skin permeation, and in vivo efficacy will help to confirm and extend the current results. Overall, these results provide a strong foundation for the development of an efficient topical antifungal delivery system.

Conclusion

ITZ-loaded PLGA nanoparticles were successfully prepared using the nanoprecipitation method and were systemically optimized to form a novel drug delivery system with potential for topical delivery. Collectively, these findings suggest that the optimized ITZ-loaded PLGA nanoparticles have favorable characteristics and features that make them a promising delivery system for topical administration of itraconazole. However, future in vivo and clinical studies are needed to confirm and extend the current findings and the potential of the ITZ-loaded PLGA nanoparticles for topical antifungal therapy.

ACKNOWLEDGMENTS

The authors thank the University of Sulaimani for for providing the necessary facilities to conduct this study.

Conflict of interests

The authors declared no conflict of interest.

Funding source

The authors did not receive any source of funds.

Data sharing statement

Supplementary data can be shared with the corresponding author upon reasonable request.

REFERENCES

1. Bootman JL. Cost-effectiveness of two new treatments for onychomycosis: An analysis of two comparative clinical trials. *J Am Acad Dermatol*. 1998;38(5, Supplement 2):S69-S72. doi: 10.1016/S0190-9622(98)70488-8.
2. Islam TAB, Majid F, Ahmed M, Afrin S, Jhumky T, Ferdouse F. Prevalence of dermatophytic infection and detection of dermatophytes by microscopic and culture methods. *J Enam Med Coll*. 2018;8(1):11-15. doi: 10.3329/jemc.v8i1.35429.
3. Kumar N, Goindi S. Statistically designed nonionic surfactant vesicles for dermal delivery of itraconazole: Characterization and in vivo evaluation using a standardized Tinea pedis infection model. *Int J Pharm*. 2014;472(1):224-240. doi: 10.1016/j.ijpharm.2014.06.030.
4. Dhakane SS, Pandit AP. Novel itraconazole nano-spanlastics gel with enhanced penetration to treat topical fungal infection. *J Drug Deliv Sci Technol*. 2023;90:105093. doi: 10.1016/j.jddst.2023.105093.
5. Chen Y, Feng X, Meng S. Site-specific drug delivery in the skin for the localized treatment of skin diseases. *Expert Opin Drug Deliv*. 2019;16(8):847-867. doi: 10.1080/17425247.2019.1645119.
6. El-Housiny S, Shams Eldeen MA, El-Attar YA, Salem HA, Attia D, Bendas ER, et al. Fluconazole-loaded solid lipid nanoparticles topical gel for treatment of pityriasis versicolor: formulation and clinical study. *Drug Deliv*. 2018;25(1):78-90. doi: 10.1080/10717544.2017.1413444
7. Mathur M, Devi VK. Potential of novel drug delivery systems in the management of topical candidiasis. *J Drug Target*. 2017;25(8):685-703. doi: 10.1080/1061186x.2017.1331352

8. Goyal R, Macri LK, Kaplan HM, Kohn J. Nanoparticles and nanofibers for topical drug delivery. *J Control Release*. 2016;240:77-92. doi: 10.1016/j.jconrel.2015.10.04.
9. Jain RK. Delivery of molecular and cellular medicine to solid tumors. *Adv Drug Deliv Rev*. 2001;46(1-3):149-168. doi: 10.1016/s0169-409x(00)00131-9.
10. Wang AZ, Langer R, Farokhzad OC. Nanoparticle delivery of cancer drugs. *Annu Rev Med*. 2012;63:185-198. doi: 10.1146/annurev-med-040210-162544.
11. Abbott LC, Maynard AD. Exposure assessment approaches for engineered nanomaterials. *Risk Anal*. 2010;30(11):1634-644. doi: 10.1111/j.1539-6924.2010.01446.x.
12. Abdelhalim MA. Gold nanoparticles administration induces disarray of heart muscle, hemorrhagic, chronic inflammatory cells infiltrated by small lymphocytes, cytoplasmic vacuolization and congested and dilated blood vessels. *Lipids Health Dis*. 2011;10:233. doi: 10.1186/1476-511x-10-233.
13. Dey S, Mazumder B, Pathak Y, (Eds.), Models for risk assessments of nanoparticles, 2014. p. 383-424. doi: 10.1201/b17191-20.
14. Grognet JM. Nanotechnologies: from information sciences to pharmacology. *Therapie*. 2008;63(1):1-9. doi: 10.2515/therapie:2008003.
15. Desai MP, Labhasetwar V, Amidon GL, Levy RJ. Gastrointestinal uptake of biodegradable microparticles: effect of particle size. *Pharm Res*. 1996;13(12):1838-1845. doi: 10.1023/a:1016085108889.
16. Alhowyan AA, Altamimi MA, Kalam MA, Khan AA, Badran M, Binkhathlan Z, et al. Antifungal efficacy of Itraconazole loaded PLGA-nanoparticles stabilized by vitamin-E TPGS: In vitro and ex vivo studies. *J Microbiol Methods*. 2019;161:87-95. doi: 10.1016/j.mimet.2019.01.020.
17. Patel NR, Damann K, Leonardi C, Sabliov CM. Itraconazole-loaded poly(lactic-co-glycolic) acid nanoparticles for improved antifungal activity. *Nanomedicine (Lond)*. 2010;5(7):1037-1050. doi: 10.2217/nnm.10.68.
18. Govender T, Stolnik S, Garnett MC, Illum L, Davis SS. PLGA nanoparticles prepared by nanoprecipitation: drug loading and release studies of a water soluble drug. *J Controll Rel*. 1999;57(2):171-85. doi: 10.1016/S0168-3659(98)00116-3.
19. Essa S, Louhichi F, Raymond M, Hildgen P. Improved antifungal activity of itraconazole-loaded PEG/PLA nanoparticles. *J Microencapsul*. 2013;30(3):205-217. doi: 10.3109/02652048.2012.714410.
20. Zhang Y, Huo M, Zhou J, Zou A, Li W, Yao C, et al. DDSolver: an add-in program for modeling and comparison of drug dissolution profiles. AAPS J. 2010;12(3):263-271. doi: 10.1208/s12248-010-9185-1.
21. Zuo J, Gao Y, Bou-Chacra N, Löbenberg R. Evaluation of the DDSolver software applications. *Biomed Res Int*. 2014;2014:204925. doi: 10.1155/2014/204925.
22. Gamal A, Saeed H, El-Ela FIA, Salem HF. Improving the antitumor activity and Bioavailability of sonidegib for the treatment of skin cancer. *Pharmaceutics*. 2021;13(10):1560. doi: 10.3390/pharmaceutics13101560.
23. Ekambaram P, Abdul HS. Formulation and evaluation of solid lipid nanoparticles of ramipril. *J Young Pharm*. 2011;3(3):216-220. doi:10.4103/0975-1483.83765.
24. Kedar U, Phutane P, Shidhaye S, Kadam V. Advances in polymeric micelles for drug delivery and tumor targeting. Nanomedicine. 2010;6(6):714-729. doi: 10.1016/j.nano.2010.05.005.
25. Sawant KK, Dodiya SS. Recent advances and patents on solid lipid nanoparticles. *Recent Pat Drug Deliv Formul*. 2008;2(2):120-135. doi: 10.2174/187221108784534081.
26. Quaglia F, Ostacolo L, Mazzaglia A, Villari V, Zaccaria D, Sciortino MT. The intracellular effects of non-ionic amphiphilic cyclodextrin nanoparticles in the delivery of anticancer drugs. *Biomaterials*. 2009;30(3):374-382. doi: 10.1016/j.biomaterials.2008.09.035.
27. de la Calle I, Soto-Gómez D, Pérez-Rodríguez P, López-Periago JE. Particle size characterization of Sepia ink eumelanin biopolymers by SEM, DLS, and AF4-MALLS: A comparative study. *Food Anal Methods*. 2019;12(5):1140-1151. doi: 10.1007/s12161-019-01448-0.
28. Magenheim B, Levy MY, Benita S. A new in vitro technique for the evaluation of drug release profile from colloidal carriers - ultrafiltration technique at low pressure. *Int J Pharm*. 1993;94(1):115-123. doi: 10.1016/0378-5173(93)90015-8.
29. Keles H, Naylor A, Clegg F, Sammon C. Investigation of factors influencing the hydrolytic degradation of single PLGA microparticles. *Polymer Degrad Stability*. 2015;119:228-241. doi: 10.1016/j.polymdegradstab.2015.04.025.
30. Baggi R, Kilaru N. Calculation of predominant drug release mechanism using Peppas-Sahlin model, Part-I (substitution method): A linear regression approach. *Asian J Pharm Technol*. 2016;6:223. doi: 10.5958/2231-5713.2016.00033.7.
31. Peppas NA, Sahlin JJ. A simple equation for the description of solute release. III. Coupling of diffusion and relaxation. Int J Pharm. 1989;57(2):169-172. doi: 10.1016/0378-5173(89)90306-2.